

Phase diagram of the lattice $SU(2)$ Higgs model

C. Bonati, G. Cossu, M. D'Elia, A. Di Giacomo

Abstract

We perform a detailed study of the phase diagram of the lattice Higgs $SU(2)$ model with fixed Higgs field length. Consistently with previsions based on the Fradkin-Shenker theorem we find a first order transition line with an endpoint whose position we determined. The diagram also shows cross-over lines: the cross-over corresponding to the pure $SU(2)$ bulk is also present at nonzero coupling with the Higgs field and merges with the one that continues the line of first order transition beyond the critical endpoint. At high temperature the first order line becomes a crossover, whose position moves by varying the temperature.

1 Introduction

In this work we present a detailed study of the phase diagram of the lattice Higgs $SU(2)$ model with Higgs field in the fundamental representation and of fixed length¹. The model in which Higgs length is allowed to change has received quite a lot of attention in the past for its possible phenomenological implications (see e.g. [2]), so that its phase diagram is known with good precision. No systematic study exists instead for the case in which the Higgs length is frozen. However this last model is often used, mainly because of its computational simplicity in numerical simulations, as the prototype of a non-Abelian gauge theory coupled with matter in the fundamental representation. In particular some work has been done to study confinement in this model ([3] and [4]). In those works some properties of the phase diagram are usually taken for granted, like the existence of a line of first order transitions for $\beta \gtrsim 2.3$, but they have never really been tested in simulations. As a first step towards a complete understanding of this model, we thus started to systematically investigate its phase diagram, in order to obtain precise estimates of the location of its critical points.

The action of lattice Higgs $SU(2)$ model we adopt is

$$S = \beta \sum_{x,\mu<\nu} \left\{ 1 - \frac{1}{2} \text{ReTr} P_{\mu\nu}(x) \right\} - \frac{\kappa}{2} \sum_{x,\mu>0} \text{Tr}[\phi^\dagger(x) U_\mu(x + \hat{\mu}) \phi(x + \hat{\mu})] \quad (1)$$

where the first term is the standard Wilson action and the Higgs field ϕ (which transforms in the fundamental representation) is rewritten as an $SU(2)$ matrix (see e.g. [5], [6]). Since the action is linear in the fields at each point, standard heatbath ([7], [8]) and overrelaxation ([9]) algorithms can be used for the Monte Carlo update. If the Higgs length is allowed to change this is no longer true, since

¹A first report of this study was presented at the LATTICE 2008 conference, [1].

in this case a quartic term is needed, which has the form $\lambda\{\frac{1}{2}\text{Tr}[\phi^\dagger(x)\phi(x)]-1\}^2$ and destroys linearity.

In the limit $\beta \rightarrow \infty$ the theory reduces to an $O(4)$ non-linear sigma model, which is known to have a mean field phase transition for $\kappa \approx 0.6$ (see e.g. [10]); in [11] it was shown that this second order transition becomes a first order *à la* Coleman-Weinberg when the gauge field is introduced as a small perturbation (β large). The authors of [11], using the cluster expansion developed in [12], were also able to prove the existence of a region of parameter space near the axis $\beta = 0$ and for $\kappa \rightarrow \infty$ where *every local observable is analytic*. This statement is often referred to as the Fradkin-Shenker (FS) theorem. It is important to notice that, in this context, an observable is defined as local when its support is contained in a compact set in the thermodynamic limit; observables not satisfying this requirement can have non-analytic behaviour (see e.g. [13, 14]). This two results suggest a phase diagram like that shown in Fig. 1: the analyticity region is indicated by AR and is limited by the dotted line, the thick line is the line of first order transitions and the two dots are its second order endpoints. As long as we consider the model at zero temperature, the ϵ -expansion predicts the endpoints to be in the mean field universality class.

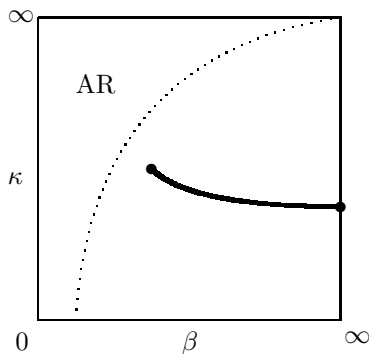


Figure 1: Phase diagram of the Higgs $SU(2)$ model as predicted in [11].

A similar phase diagram was observed in the works [2], [15] for the lattice Higgs $SU(2)$ model with fourth-order scalar coupling $\lambda \leq 0.5$, while in the model considered here $\lambda \rightarrow \infty$. Because of the supposed triviality of the ϕ^4 model in four dimensions, λ is expected to be a marginally irrelevant parameter and therefore the phase diagram not to change qualitatively for $\lambda \rightarrow \infty$ (see e.g. [16]); however it was observed since long time that the first order transition gets weaker as λ is increased, so that the phase diagram of Fig. 1 has not really been checked at large values of λ .

After the seminal work ref. [17] on very small lattices, in ref. [18] the observation of a double peak structure was reported at $\beta = 2.3$ on a 16^4 lattice, which however was probably only a consequence of the poor statistics, since in a later study, ref. [19], no double peak was found at $\beta = 2.3$. There it was stated that “the system exhibits a transient behaviour up to $L = 24$ along which the order of the transition cannot be discerned”. In this paper we produce the first clear evidence of the line of first order transition and we obtain an estimate of the endpoint position.

2 Numerical results

The obvious observables to look at for this system are

- the gauge-Higgs coupling, $G = \frac{1}{2} \langle \text{Tr}[\phi^\dagger(x) U_\mu(x + \hat{\mu}) \phi(x + \hat{\mu})] \rangle$
- the plaquette, $P = \frac{1}{2} \langle \text{Tr} P_{\mu\nu} \rangle$
- the energy density $E = 6\beta P + 4\kappa G$

Besides these natural ones, we monitored also the following observables:

- the Polyakov loop $P_L(\vec{x}) = \frac{1}{2} \text{Tr} \left[\prod_{t=0}^{L_t-1} U_0(t, \vec{x}) \right]$, $P_L = \frac{1}{V} \langle \sum_{\vec{x}} P_L(\vec{x}) \rangle$
- the Z_2 monopoles density, $M = 1 - \frac{1}{N_c} \sum_c \sigma_c$, where c stand for the elementary cube and $\sigma_c = \prod_{P_{\mu\nu} \in \partial c} \text{sign Tr} P_{\mu\nu}$

The Polyakov loop behaviour is used as an indicator of confinement. The study of the Z_2 monopoles is motivated by the similarity of the first order transition with the bulk transition of the $SU(2)$ pure gauge theory, which is driven by lattice artefacts such as the Z_2 monopoles. Both these points will be discussed more accurately in the following.

Data were analyzed by using the optimized histogram method ([20]) and the statistical errors were estimated by using the moving block bootstrap method (see e.g. [21]).

The presentation of the simulation results will be divided in several parts

1. we will show that at $\beta = 2.5$ there is no signal of a phase transition and data are consistent with a smooth cross-over
2. we will show that for $\beta \geq 2.775$ the scaling is consistent with a first order transition and we will present evidence of a double peak structure
3. two independent estimates of the endpoint will be obtained
4. we will give hints that the above transitions are not related to confinement
5. we will investigate the relation between the line of first order transition, which becomes a smooth cross-over beyond the endpoint, and the pure $SU(2)$ bulk transition
6. finally we will present some exploratory results at $T \neq 0$

All results in the first four parts have been obtained by fixing the value of β and by looking for transitions in κ .

2.1 Cross-over region

In Fig. 2 the maxima of the susceptibilities of G , P and M are plotted for various lattice sizes and $\beta = 2.5$. For lattices up to $L \approx 18$ the maxima of susceptibilities are well described by a function of the form $a + bL^4$, so that they seem to scale linearly with volume as expected for a first order transition. However on larger lattices all susceptibilities saturate and no singularity seems to develop in the thermodynamical limit. This means that the system has a

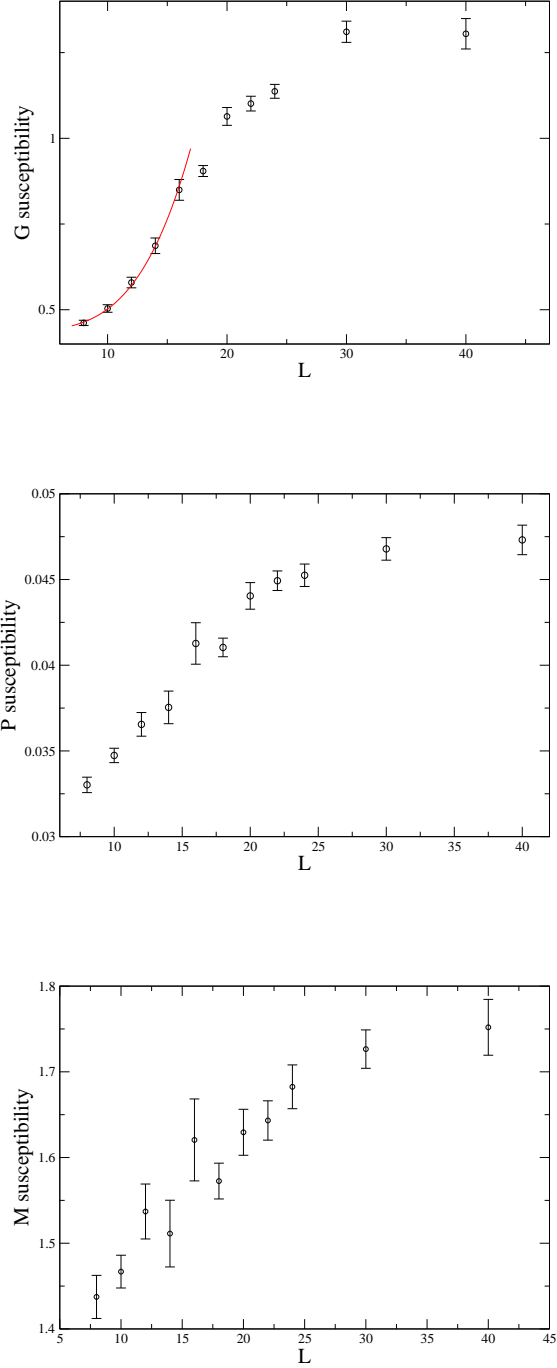


Figure 2: *Top:* G susceptibility peak heights at $\beta = 2.5$ (the continuous line is a fit to $a + bx^4$). *Center:* P susceptibility peak heights at $\beta = 2.5$. *Bottom:* M susceptibility peak heights at $\beta = 2.5$. Clearly they all saturate at large L .

correlation length of order ≈ 10 lattice spacing, so that the increase of the susceptibilities with volume, that in previous studies was interpreted as due to a first order transition, is just a signal that the lattices were too small.

To look for transitions, besides susceptibilities we also check the behaviour of the energy Binder cumulant, which is defined as $B = 1 - \langle E^4 \rangle / (3 \langle E^2 \rangle^2)$. It can be shown (see e.g. [22]) that near a transition B develops minima whose depth scales as

$$B|_{min} = \frac{2}{3} - \frac{1}{12} \left(\frac{E_+}{E_-} - \frac{E_-}{E_+} \right)^2 + O(L^{-4}) = \frac{2}{3} - \frac{1}{3} \left(\frac{\Delta}{\epsilon} \right)^2 + O(\Delta^3) + O(L^{-4}) \quad (2)$$

where $E_{\pm} = \lim_{\beta \rightarrow \beta_c^{\pm}} \langle E \rangle$, $\Delta = E_+ - E_-$ and $\epsilon = \frac{1}{2}(E_+ + E_-)$. In particular the thermodynamical limit of $B|_{min}$ is less than $2/3$ if and only if a latent heat is present.

The scaling of the energy Binder cumulant minima at $\beta = 2.5$ is shown in Fig. 3. Also here two different behaviours are clearly visible: on small lattices there is scaling consistent with a first order transition. By increasing the volume $B \rightarrow 2/3$, indicating a smooth cross-over or a second order transition.

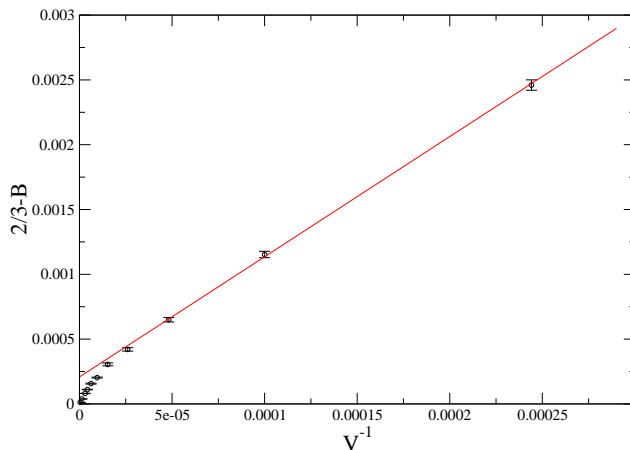


Figure 3: Binder cumulant minima of E at $\beta = 2.5$ ($V = L^4$).

These results indicate that at $\beta = 2.5$ there is no transition; this is in sharp contrast with all previous studies of this model, which concluded that for $\beta \geq 2.3$ the system undergoes a first order transition. This wrong conclusion was based on the analysis of lattices of size up to 25^4 , which we have just shown to be too small.

2.2 First order region

At $\beta = 2.775$, $\beta = 2.79$ and $\beta = 2.8$ the scaling of the susceptibilities and of the energy Binder cumulant remains consistent with first order also for the

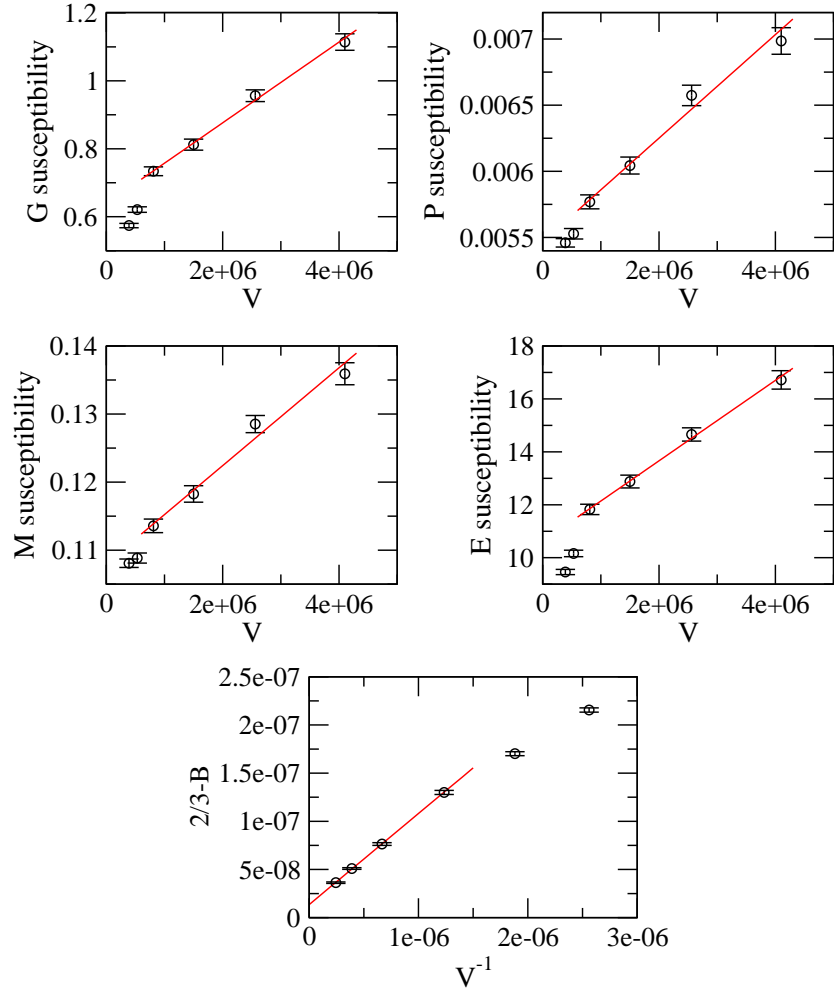


Figure 4: Scaling of the maxima of the susceptibilities and of the E Binder cumulant minima for $\beta = 2.775$ ($V = L^4$ and the larger V values correspond to lattice sizes $L = 30, 35, 40, 45$).

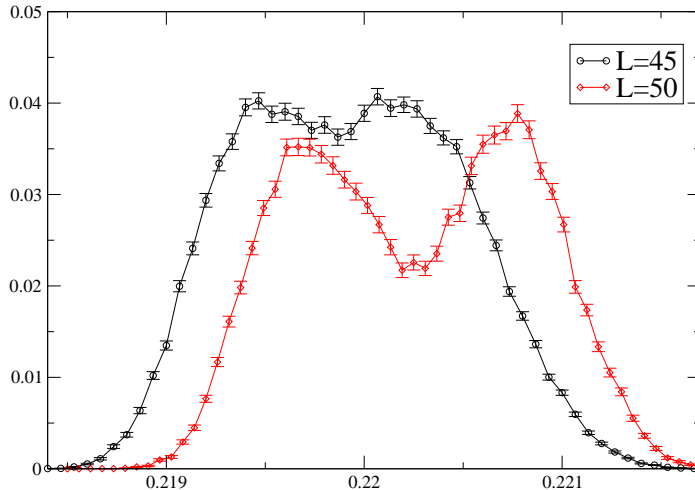


Figure 5: Histogram of the observable G for $\beta = 2.8$ on the two largest lattices.

larger lattices, as shown for example in Fig. 4 for $\beta = 2.775$. In this range of β values the transition gets stronger as β increases. However we know that the transition at $\beta \rightarrow \infty$ has to become of second order, so that going at β high enough the transition has to get weaker. We could not reach this regime in our simulations since when increasing the β value it is also necessary to use larger lattices. To have results free of spurious finite size transitions the lattice must be large enough for the corresponding pure $SU(2)$ gauge theory to be confined and exponentially large lattices in β are needed.

Although all observables scale consistently with a first order transition, a clear signal of metastability was revealed only at $\beta = 2.8$, where the transition is stronger, and only in the two largest lattices, namely $L = 45$ and $L = 50$; the histograms for the observable G on these two lattices are shown in Fig. 5, where the formation of a double peak structure is visible.

2.3 Endpoint

Having three sets of data with first order scaling and knowing the universality class of the endpoint, we can estimate its position β_c assuming that we are close enough to it. We can do this in two independent ways:

1. From the second form of equation 2 we know the dependence of B on the discontinuity Δ and for a mean-field transition we have $\Delta \propto t^{1/2}$, where t is the reduced temperature, $t = (T - T_c)/T_c$. In our case, near the critical

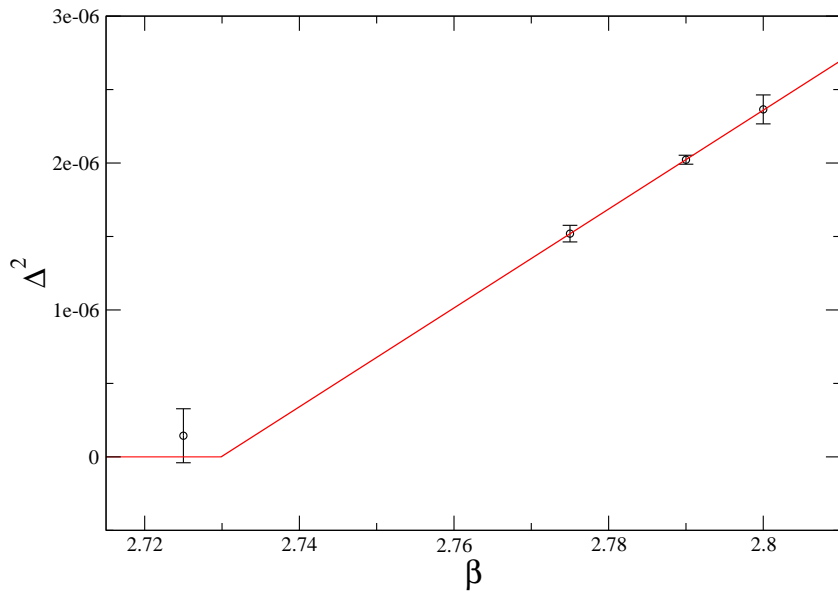
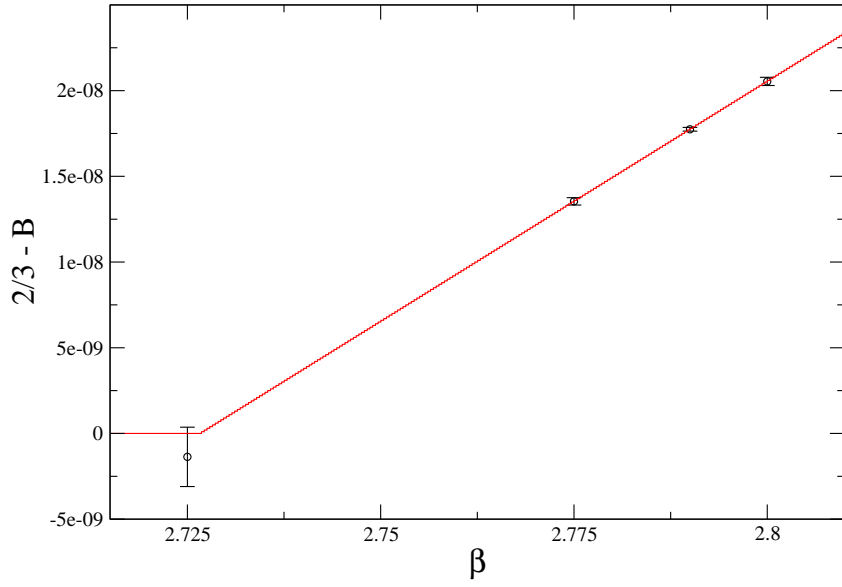


Figure 6: *Top*: Determination of the critical point using the method (1). *Bottom*: Determination of the critical point using the method (2).

point, we can use $t \propto (\beta - \beta_c)$ and therefore equation 2 can be written as²

$$\lim_{L \rightarrow \infty} B_L|_{min} = \frac{2}{3} - \gamma_1(\beta - \beta_c) + O(\beta - \beta_c)^2 \quad (3)$$

2. For a first order transition the susceptibilities scale for large volume as

$$\chi = V(\langle O^2 \rangle - \langle O \rangle^2) \approx \text{const} + V\Delta^2 \quad (4)$$

so that fitting the χ maxima to the relation $\chi = \text{const} + V\Delta^2$ and using again $\Delta \propto t^{1/2}$, we obtain

$$\Delta^2 = \gamma_2(\beta - \beta_c) + O(\beta - \beta_c)^2 \quad (5)$$

The fit in the planes (β, B) and (β, Δ^2) are shown in Fig. 6 (we use the G susceptibility); in both cases the fit is very good and the estimates for the critical point position are

$$\beta_c^{(1)} = 2.7266(16) \quad \beta_c^{(2)} = 2.7299(36) \quad (6)$$

which agree with each other within errors.

2.4 Relation to confinement

The next question is to understand if the two “phases” found at large β have different confinement properties. We recall that they cannot be considered as different thermodynamical phases as a consequence of FS theorem.

In this model Wilson loops never obey the area law because of the presence of the Higgs field, which destroys the center symmetry of the pure gauge theory; as a consequence the Polyakov loop is always non-zero (a direct check of this is shown in Fig.8) and cannot be an order parameter. Nevertheless Polyakov loop is commonly used as a confinement tracker also in theories where it is not an order parameter, e.g. in QCD, since it abruptly jumps at the deconfinement transition. For the lattice $SU(2)$ Higgs model the Polyakov loop doesn't seem to be influenced in any way by the transition: for small lattices it slightly increases, however for larger ones, the transition gets stronger but P_L gets flatter in the transition region, as can be seen in Fig. 8 (the transition is at $\kappa = 0.704675(30)$). Also Polyakov loop correlators, measured by using the multilevel algorithm of ref. [24], do not show any significant change across the transition, as shown in the bottom of Fig. 8.

An alternative possibility is to use the order parameter introduced in [25], which we will denote by O_{FM} . This is defined by the limit for $R \rightarrow \infty$ of the quantity $O_{FM}(R)$, which is constructed as the square of the mean value of a staple-shaped parallel transport connecting two Higgs fields divided by a Wilson loop; the size of the staple is related to that of the Wilson loop as shown in Fig. 7, where Higgs fields are represented by dots. To our knowledge O_{FM}

²A subtlety has to be considered here: since in this model the two relevant operators at the mean field critical point are not related to any symmetry of the system, there is in general mixing between the magnetic and thermal relevant operators (see e.g. [23]). However, since the Δ 's are measured along the coexistence curve, near the critical endpoint the mixing is negligible and the relation between Δ and t is as usual $\Delta \propto t^\beta$ (here “ β ” is the β critical exponent).

$$O_{FM}(R) = \frac{\langle R \updownarrow \overbrace{\hspace{2R}}^{2R} \rangle^2}{\langle \overbrace{\hspace{2R}}^{2R} \square \overbrace{\hspace{2R}}^{2R} \rangle}$$

Figure 7: $O_{FM}(R)$ definition.

has never been measured in a Monte Carlo simulation, so we have no previous results to compare with; its strong coupling limit was computed in [26]. $O_{FM}(R)$ measures the overlap between a Higgs-Higgs dipole of linear dimension R and the vacuum; if asymptotic colored states exist they are orthogonal to the vacuum, so $O_{FM}(R) \rightarrow 0$ for $R \rightarrow \infty$, otherwise we must have $O_{FM}(R) \rightarrow \alpha > 0$. The results obtained by measuring $O_{FM}(R)$ on a 40^4 lattice at $\beta = 2.775$ for κ slightly above and slightly below the transition points are shown in Fig. 9, where the two lines are fits to the function³ $f(x) = a + b\frac{1}{x^c}$ (symmetrized because of periodic boundary condition).

We have for the parameter a , c the estimates:

$$a_{(0.7046)} = 4.9(1) \cdot 10^{-5} \quad c_{(0.7046)} = 2.98(5) \quad (7)$$

$$a_{(0.7048)} = 10.5(5) \cdot 10^{-5} \quad c_{(0.7048)} = 3.30(23) \quad (8)$$

so on both sides of the transition charge is screened and according to the interpretation of [25] there is color confinement.

2.5 The pure gauge $SU(2)$ bulk

Another interesting point to study is what relation (if any) the first order has with the bulk transition of the $SU(2)$ pure gauge (we call this “transition” for the sake of simplicity, although it is only a rapid but smooth cross-over). An hint on the existence of such a relation can be obtained by noting that the value $\beta \approx 2.3$ previously thought to be the first order line endpoint position is the value of the bulk $SU(2)$ transition.

Since some test simulations indicated that the position of the $SU(2)$ bulk is very stable for small values of κ (so that in the plane (β, κ) this crossover follows a line perpendicular to the β axis), it seems more convenient to hold κ fixed and vary the β value; the results obtained on a 30^4 lattice for the plaquette susceptibilities for several κ values are shown in Fig. 10.

From these data a structure of cross-over lines emerges as shown in Fig. 11. For $\kappa < 0.6$ the bump in β of the plaquette susceptibility which corresponds to the $SU(2)$ bulk transition is independent on κ both in position and in shape (vertical dotted line in Fig. 11). For κ larger than 0.6 two peaks in β appear, the bulk one and the first order transition studied above. The latter peak persists also when κ is greater than the critical value corresponding to the endpoint

³This ansatz is motivated by the observation that for R big enough such that the Wilson loop scales with perimeter, the exponentials in numerator and denominator are the same, leaving a power law.

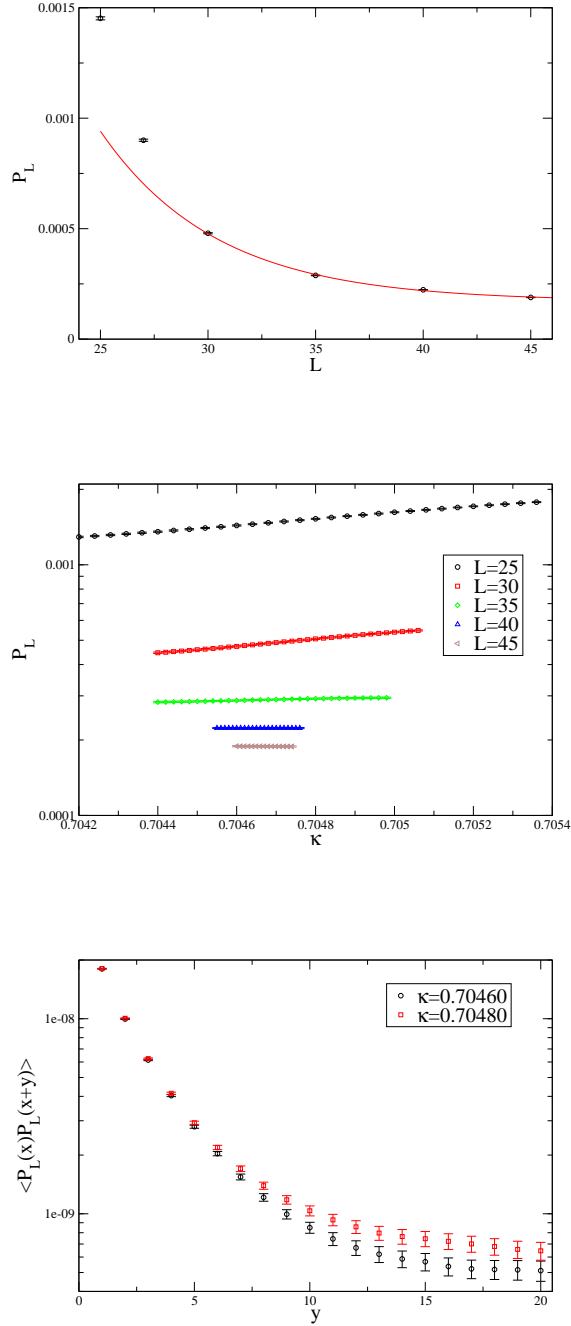


Figure 8: *Top*: Polyakov loop for $\beta = 2.775$, $\kappa = 0.70464$ and various L , the line is a fit to $a + b \exp(-cL)$ and the result for the asymptotic value is $a = 1.7(1) \cdot 10^{-4}$. *Center*: Polyakov loop for $\beta = 2.775$ and various L . *Bottom*: Polyakov loop correlators measured on a 40^4 lattice for $\beta = 2.775$ and κ slightly below (0.7046) and above (0.7048) the critical value.

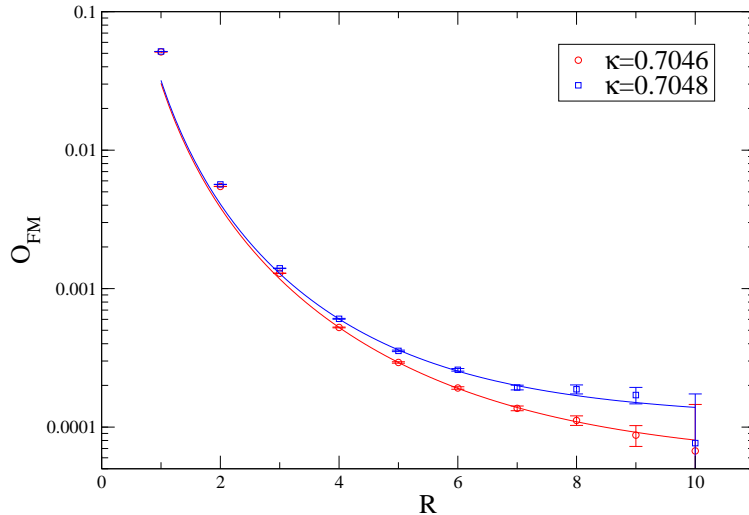


Figure 9: Results for $O_{FM}(R)$ at $\beta = 2.775$ on a 40^4 lattices slightly above and below the transition point.

and there is no real transition, although it is smaller than the $SU(2)$ bulk signal (see Fig. 10, $\kappa = 0.75$). By increasing the κ value the cross-over remnant of the first order transition moves towards smaller β values, until it intersects the $SU(2)$ bulk in the point indicated by A in Fig. 11. In the neighborhood of the point A the “first order continuation” peak gets stronger and the $SU(2)$ bulk disappears. This increase could have been misinterpreted as the first order transition line endpoint in previous works. A direct check to ensure that in this region there is no transition is shown in Fig. 12. For still larger κ values only one maximum is present in susceptibilities, which gets weaker as $\kappa \rightarrow \infty$.

This interplay between the first order transition line and the bulk $SU(2)$ suggests that the first order transition could be in some way related to the same lattice artifacts that drive the bulk $SU(2)$ transition, namely the Z_2 monopoles. The density of Z_2 monopoles seems indeed to have a jump across the transition (see Fig. 4).

2.6 Finite temperature

Motivated by the last observation we try to investigate if the first order transition line can itself be thought as a lattice artefact, like the pure gauge $SO(3)$ first order bulk transition. To answer this question the simplest method is to consider the system at finite temperature: bulk transitions are insensitive to the temporal extension L_t of the lattice, while physical transitions scale by varying L_t .

For each L_t value we simulate the system with several spatial extents L_s , in

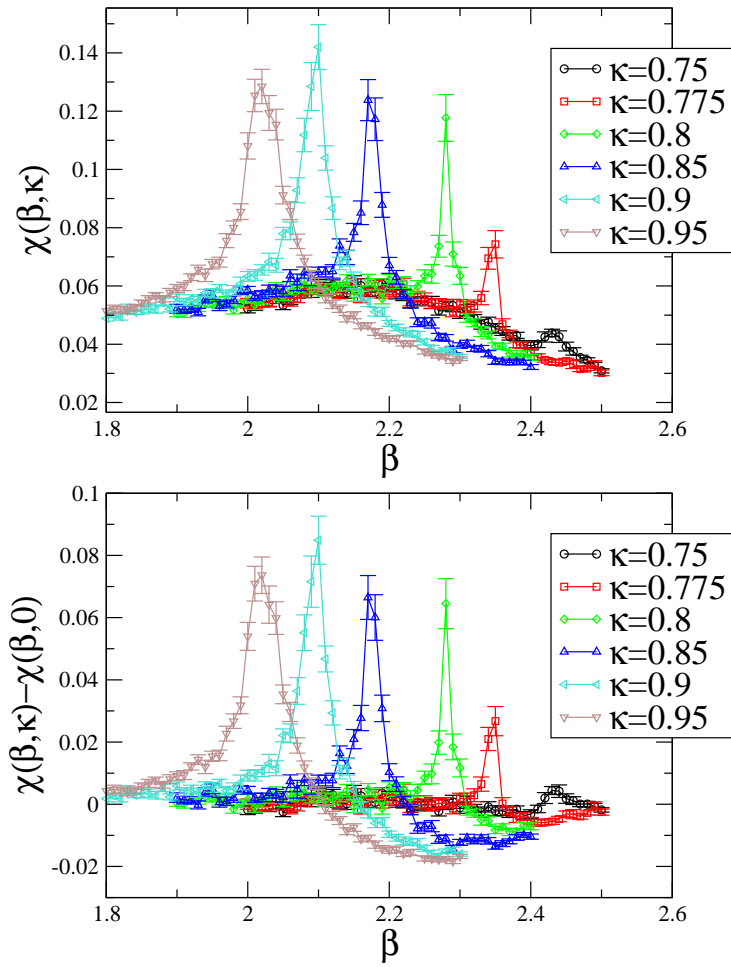


Figure 10: *Up*: plaquette susceptibility. *Down*: plaquette susceptibility with subtracted the value at $\kappa = 0$.

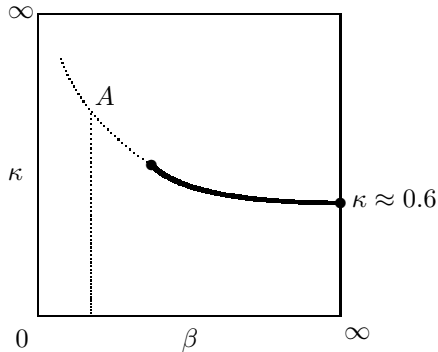


Figure 11: Phase diagram of the Higgs $SU(2)$ with rapid crossovers indicated by dotted lines.

order to perform a finite size analysis. Some of the results obtained are shown in Fig. 13. It is clear that the position of the maxima of the G susceptibility moves by varying L_t , so that the line of first order transition seen at zero temperature cannot be a lattice artifact. Moreover for all the values of L_t considered the maxima saturate by increasing L_s , indicating the absence of a phase transition. We expect that for sufficiently small temperature (i.e. large enough L_t) the first order transition is restored, however to observe this behaviour numerically we should use lattices with $L_t > 20$ and $L_s \gg L_t$, typically $L_s \gtrsim 3L_t$. Instead we have to restrict ourselves to $L_s^3 L_t \lesssim 4 \times 10^6$ because of computer capability. In any case we see the cross-over gets stronger by increasing the lattice temporal extension.

3 Conclusions

This paper is a study of the phase diagram of the $SU(2)$ Higgs gauge theory with the Higgs in the fundamental representation and fixed length. We find that to investigate the phase structure of this system it is necessary to use much larger lattices than the ones adopted in the past due to the large correlation length.

We present the first clear evidence of the presence of a line of first order transition and we estimate its endpoint position to be at $\beta_c = 2.7266(16)$, thus confirming an expectation based on the Fradkin-Shenker theorem.

We give indications that this transition is not a deconfinement transition.

We attempt an exploration of the system at finite temperature; the first order transition becomes then a cross-over whose position moves by varying the temperature.

4 Acknowledgments

Simulation were performed using the Italian GRID Infrastructure and one of us (C. B.) wishes to thank Tommaso Boccali for his technical assistance in its use. We thank A. D'Alessandro for substantial help in the early stages of this work.

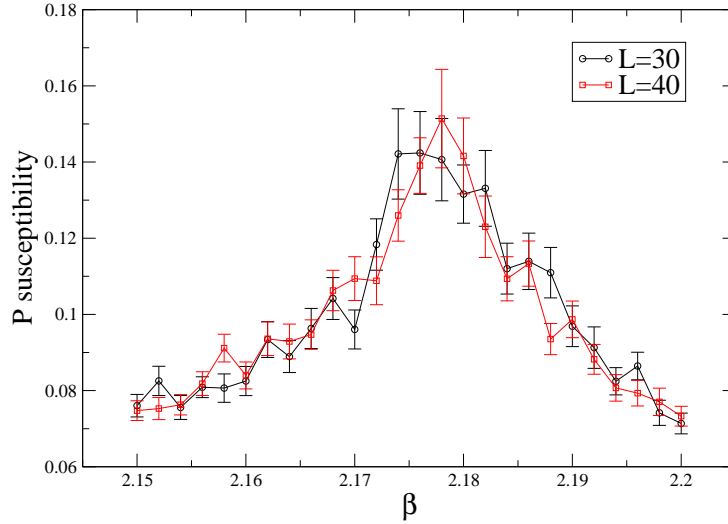


Figure 12: Plaquette susceptibility for $\kappa = 0.85$.

A Data

In this appendix we give some details of our numerical results. The notation is as follows

- κ_{pc} is the location in κ of the G susceptibility maximum
- χ_O is the peak value of the susceptibility of the O observable
- B is the value at minimum of the energy Binder cumulant

$\beta = 2.725$						
L	κ_{pc}	χ_G	χ_P	χ_M	χ_E	$2/3-B$
20	0.7090(2)	0.615(18)	0.005575(88)	0.1147(19)	10.85(30)	6.36(18)e-07
25	0.7089(2)	0.692(16)	0.005831(71)	0.1194(15)	11.89(26)	2.839(62)e-07
30	0.7088(1)	0.858(20)	0.006485(78)	0.1319(15)	14.51(32)	1.679(38)e-07
35	0.70873(5)	1.018(24)	0.007082(89)	0.1431(17)	16.64(37)	1.039(23)e-07
40	0.70866(5)	1.022(24)	0.00704(12)	0.1426(18)	16.85(37)	6.17(13)e-08
45	0.70886(5)	0.994(31)	0.00725(23)	0.1469(25)	16.25(47)	3.71(10)e-08

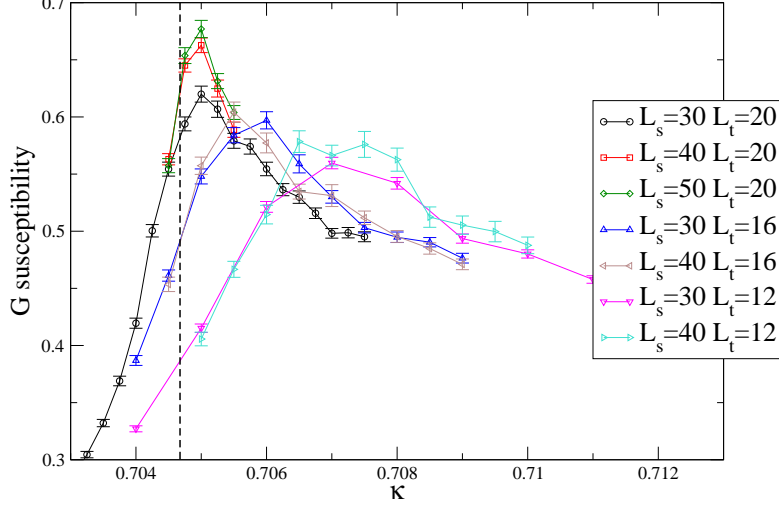


Figure 13: G susceptibility for $\beta = 2.775$; the vertical line indicates the place where on symmetric lattices the transition is observed.

$\beta = 2.775$						
L	κ_{pc}	χ_G	χ_P	χ_M	χ_E	$2/3-B$
25	0.7049(1)	0.5740(65)	0.005459(31)	0.10807(62)	9.460(98)	2.156(22)e-07
27	0.70480(8)	0.6211(82)	0.005528(40)	0.10884(74)	10.16(12)	1.702(21)e-07
30	0.70476(5)	0.734(13)	0.005769(52)	0.1135(10)	11.82(19)	1.299(21)e-07
35	0.70466(5)	0.812(16)	0.006044(64)	0.1182(12)	12.88(24)	7.64(14)e-08
40	0.70469(3)	0.956(17)	0.006573(77)	0.1285(12)	14.66(25)	5.099(88)e-08
45	0.704675(30)	1.114(24)	0.00698(10)	0.1359(16)	16.72(34)	3.631(75)e-08

$\beta = 2.79$						
L	κ_{pc}	χ_G	χ_P	χ_M	χ_E	$2/3-B$
25	0.70380(10)	0.5512(97)	0.005301(48)	0.10362(93)	9.05(14)	2.030(32)e-07
30	0.70360(5)	0.646(12)	0.005481(49)	0.10632(95)	10.39(17)	1.125(19)e-07
40	0.70356(3)	0.912(19)	0.006187(78)	0.1200(13)	14.01(27)	4.799(93)e-08
45	0.703525(30)	1.140(23)	0.006901(97)	0.1318(15)	17.01(33)	3.639(70)e-08

$\beta = 2.8$						
L	κ_{pc}	χ_G	χ_P	χ_M	χ_E	$2/3-B$
25	0.7032(2)	0.683(22)	0.005080(80)	0.0978(15)	11.25(34)	2.500(75)e-07
30	0.70298(8)	0.7212(85)	0.005279(38)	0.10181(60)	11.63(13)	1.246(13)e-07
35	0.70286(5)	0.760(16)	0.005685(62)	0.1093(11)	11.64(22)	6.74(13)e-08
40	0.70282(4)	0.946(22)	0.006239(75)	0.1192(13)	14.36(31)	4.87(11)e-08
45	0.70279(3)	1.219(27)	0.007033(89)	0.1339(16)	17.75(37)	3.759(78)e-08

References

- [1] C. Bonati, G. Cossu, A. D'Alessandro, M. D'Elia, A. Di Giacomo *On the phase diagram of the Higgs $SU(2)$ model*. PoS(LATTICE2008)252 (arXiv:0901.4429).
- [2] Z. Fodor, J. Hein, K. Jansen, A. Jaster, I. Montvay *Simulating the electroweak phase transition in the $SU(2)$ Higgs model*. Nucl. Phys. B **439**, 147 (1995) (arXiv:hep-lat/9409017).
- [3] J. Greensite, Š. Olejník *Vortices, symmetry breaking, and temporary confinement in $SU(2)$ gauge-Higgs theory*. Phys. Rev. D **74**, 014502 (2006) (arXiv:hep-lat/0603024).
- [4] W. Caudy, J. Greensite *On the ambiguity of spontaneously broken gauge symmetry*, Phys. Rev. D **78**, 025018 (2008) (arXiv:0712.0999 [hep-lat]).
- [5] I. Montvay *Correlations and static energies in the standard Higgs model*. Nucl. Phys. B **269**, 170 (1986).
- [6] I. Montvay, G. Münster *Quantum fields on a lattice*. Cambridge University Press (1994).
- [7] M. Creutz *Monte Carlo study of quantized $SU(2)$ gauge theory*. Phys. Rev. D **21**, 2308 (1980).
- [8] A. D. Kennedy, B. J. Pendleton *Improved heatbath method for Monte Carlo calculations in lattice gauge theories*. Phys. Lett. B **156**, 393 (1985).
- [9] M. Creutz *Overrelaxation and Monte Carlo simulation*. Phys. Rev. D **36**, 515 (1987).
- [10] A. Hasenfratz, K. Jansen, J. Jersák, B.B. Lang, T. Neuhaus, H. Yoneyama *Study of the Four Component ϕ^4 Model*. Nucl. Phys. B **317**, 81 (1987).
- [11] E. Fradkin, S. H. Shenker *Phase diagrams of lattice gauge theories with Higgs fields*. Phys. Rev. D **19**, 3682 (1979).
- [12] K. Osterwalder, E. Seiler *Gauge Field Theories on a Lattice*. Ann. Phys. **110**, 440 (1978).
- [13] R. Bertle, M. Faber, J. Greensite, Š. Olejník *Center dominance in $SU(2)$ gauge-Higgs theory*. Phys. Rev. D **69**, 014007 (2004) (arXiv:hep-lat/0310057).
- [14] M. Grady *Reconsidering gauge-Higgs continuity*. Phys. Lett. B **626**, 161 (2005) (arXiv:hep-lat/0507037).
- [15] W. Bock, H. G. Evertz, J. Jersák, D. P. Landau, T. Neuhaus, J. L. Xu *Search for critical points in the $SU(2)$ Higgs model*. Phys. Rev. D **41**, 2573 (1990).
- [16] D. J. E. Callaway *Triviality pursuit: can elementary scalar particles exist?* Phys. Rep. **167**, 241 (1988).

- [17] C.B. Lang, C. Rebbi, M. Virasoro *The phase structure of a non-Abelian gauge Higgs field system*. Phys. Lett. B **104**, 294 (1981).
- [18] W. Langguth, I. Montvay *Two-state signal at the deconfinement-Higgs phase transition in the standard $SU(2)$ Higgs model*. Phys. Lett. B **165**, 135 (1985).
- [19] I. Campos *On the $SU(2)$ -Higgs phase transition*. Nucl. Phys. B **514**, 336 (1998) (arXiv:hep-lat/9706020).
- [20] A. M. Ferrenberg, R. H. Swendsen *Optimized Monte Carlo data analysis*. Phys. Rev. Lett. **63**, 1195 (1989).
- [21] S. Mignani, R. Rosa *The moving block bootstrap to asses the accuracy of statistical estimates in Ising model simulations*. Comp. Phys. Comm. **92**, 203 (1995).
- [22] J. Lee, J. M. Kosterlitz *Finite-size scaling and Monte Carlo simulations of first-order phase transitions*. Phys. Rev. B **43**, 3265 (1991).
- [23] N. B. Wilding *Simulation studies of fluid critical behaviour*. J. Phys.: Condens. Matter **9**, 585 (1997) (arXiv:cond-mat/9610133).
- [24] M. Luscher, P. Weisz *Locality and exponential error reduction in numerical lattice gauge theory*. JHEP **09**, 010 (2001) (arXiv:hep-lat/0108014).
- [25] K. Fredenhagen, M. Marcu *Confinement Criterion for QCD with Dynamical Quarks*. Phys. Rev. Lett. **56**, 223 (1986).
- [26] K. Holland, P. Minkowki, M. Pepe, U.-J. Wiese *Exceptional Confinement in $G(2)$ Gauge Theory*. Nucl. Phys. B **668**, 207 (2003) (arXiv:hep-lat/0302023).